# Angular Distributions of the $B^{11}(d,n)C^{12}$ Ground-State Neutrons*

OAKES AMES, GEORGE E. OWEN, AND C. D. SWARTZ
*The Johns Hopkins University, Baltimore, Maryland*
(Received January 30, 1957)

The angular distributions of the ground-state neutrons from the reaction $B^{11}(d,n)C^{12}$ have been measured in the deuteron energy range of 0.500 to 1.15 Mev. A single stilbene crystal counter was employed as a neutron detector. At a bombarding energy of 0.8 Mev the neutron angular distribution exhibits a strong forward component, while at 1.15 Mev the distribution is more isotropic. The data are consistent with an analysis based on nuclear stripping theory.

## INTRODUCTION

PREVIOUS investigations[1] of the angular distributions of the ground-state neutrons from the $B^{11}(d,n)C^{12}$ reaction in the deuteron energy range from 1.6 to 4.7 Mev have shown a backward component in addition to the customary forward component which is expected from deuteron stripping theory.[2] It has been suggested[3] that neutron stripping from the target nucleus might account for the backward component.

An investigation[4] at 0.6-Mev bombarding energy indicated that the angular distribution in this energy range was characterized by a forward throw. The present experiments study the variation of the angular distribution with energy in the range from 0.5 Mev to 1.15 Mev.

## EXPERIMENTAL ARRANGEMENT

### A. Targets

The targets were prepared from $H_3BO_3$. No attempt was made to use enriched $B^{11}$, since any neutrons from the reaction $B^{10}(d,n)C^{11}$ would not be measured by our apparatus. $B_2O_3$ was evaporated onto a copper backing. An optical flat was placed in the bell jar and the deposit on the flat gave a measure of the deposit on the copper backing. The target thickness was determined by measuring the channel spectra of the light reflected from the surface of the optical flat. The average target thickness used in these experiments was about 150 kev for 1-Mev deuterons. The average energy of the interaction was, however, much closer to the incident energy, because the total cross section of the reaction at these energies is varying as the barrier penetrability. At 1 Mev the apparent thickness of the targets was less than 50 kev.

The deuteron beams were provided by the Van de Graaff generator of the Johns Hopkins University Nuclear Laboratory.

### B. Neutron Detector

A single stilbene scintillation crystal mounted on a 6342 photomultiplier was utilized to detect the neutrons from this reaction. The preliminary runs were made with a crystal 1 cm in diameter and 5 mm in thickness. Because of the low total cross section at energies around 600 kev, it was necessary to work with the 1-cm crystal about 7 cm from the target. The final data were obtained with a stilbene crystal 2 cm in diameter and 4.3 mm in thickness. These runs were performed at a distance of 12.5 cm from the target.

In both cases it was necessary to shield the crystal from the high-energy electrons from the $B^{11}(d,p)B^{12}$-$(\beta^-)C^{12}$ reaction. A series of background checks showed that the final measurements were free from the electron background when the crystals were shielded by a lead disk one-quarter inch thick.

In addition to the electron background, there is a high-energy gamma-ray background. However, the pulses from the interaction of these gamma rays in the crystal are not high enough to cause interference in the proton recoil spectrum of the ground state neutrons of the reaction $B^{11}(d,n)C^{12}$.

It is apparent that the best results are obtained when the volume and thickness of the crystal are kept to a minimum value commensurate with the intensity of the neutrons and the range of the highest energy recoil protons.

The efficiency of the detectors has been calculated and the nonlinearity between the energy of the recoil proton and the associated pulse height has been checked with previous measurements.

The pulse-height spectra were displayed on two Atomic Instrument Company 20-channel analyzers arranged in tandem.

### C. Measurements of the Beam Intensity

The experiments were monitored by a current integration of the beam, and in a given angular distribution at a specified beam energy the relative intensities were monitored by a stilbene crystal counter which detected the electrons from the decay of $B^{12}$ to $C^{12}$, as well as the other reaction products. In most cases, for a given incident energy it was found that the ratio of current

* Supported by the U. S. Atomic Energy Commission.
[1] Class, Price, and Risser (private communication, to be published).
[2] S. T. Butler, Proc. Roy. Soc. (London) **A208**, 559 (1951); A. B. Bhatia *et al.*, Phil. Mag. **43**, 483 (1952).
[3] L. Madansky and G. E. Owen, Phys. Rev. **99**, 1608 (1955).
[4] A. Ward and P. Grant, Proc. Phys. Soc. (London) **A68**, 637 (1955).

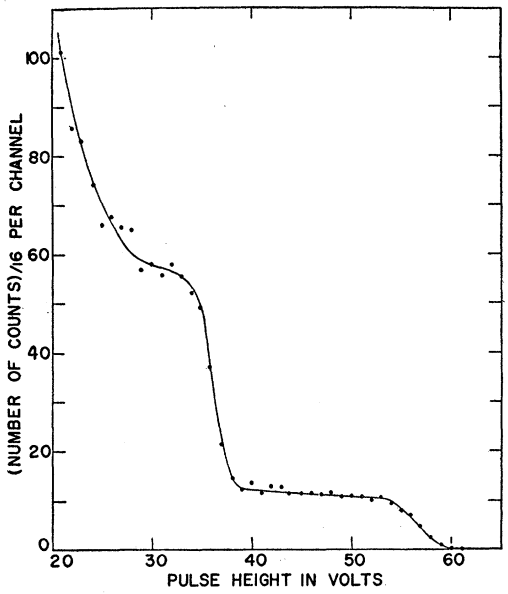


FIG. 1. Pulse-height spectrum of recoil protons from the neutrons of the $B^{11}(d,n)C^{12}$ reaction. The two steps clearly represent the recoil groups from the ground and first excited states.

integrator counts to monitor counts was constant to within 5%.

### D. Analysis of the Data

A typical pulse-height spectrum of the recoil protons from the neutrons of the $B^{11}(d,n)C^{12}$ reaction is shown in Fig. 1.

The theoretical step function which arises from the *n-p* scattering is distorted mainly by the finite resolution of the detector system, the nonlinear pulse height response of stilbene, and end effects.

It is seen in Fig. 1 that although the recoil proton spectrum corresponding to the ground state neutrons shows little distortion, the proton spectrum for the first excited state is not so well defined. The major distortion in the first excited state spectrum arises from the presence of the end point of the high-energy gamma-ray background. Since the $B^{10}$ contaminant contributes a large number of these gamma rays, it seems necessary to use enriched $B^{11}$ targets for the study of the first excited state. Also smaller crystals will discriminate against this gamma background.

The data of the ground-state neutrons were analyzed in the following manner. First the pulse-height spectrum is integrated and the number of pulses above a height $S$ is plotted against $S$. At the high proton energies involved in this reaction, the pulse height *versus* energy function is quite linear in the region near the end point, and therefore the integrated plot is a straight line except for the resolution distortion near the end point and end effects. After correcting for the end effects, the extrapolation of the straight line gives the pulse height corresponding to the end point and thus allows conversion to an energy spectrum. Once the corrected pulse-height spectrum is converted to an energy spectrum, the calculation of the neutron intensity is straightforward. An integrated energy spectrum is shown in Fig. 2.

End-effect corrections were made in all cases. This effect arises from the fact that a proton may escape from the crystal before giving up its full energy. Figure 2 shows the result of performing this correction. It should be noted that the linearity of the plot is improved. This correction must be made if total cross sections are to be obtained. Since there is not a large variation in neutron energy over a single angular distribution, the end-effect correction does not make a marked change in the shape of the angular distribution curves.

Since the data involve many different neutron energies, a check of the pulse-height nonlinearity curve was possible. The results showed agreement to better than 5%. The neutron intensity calculation is based on energy ratios; therefore the final intensity calculations are more accurate than the nonlinearity correction.

Neutron intensities were measured at the same angles on both sides of the beam axis to check the centering of the target.

## RESULTS

The angular distributions of the ground state neutrons for deuteron bombarding energies of 0.5; 0.6; 0.8; 1.00; and 1.15 Mev are shown in Fig. 3. It can be seen that the distributions are relatively isotropic in the region of 1.15 Mev and that there is a characteristic forward throw at lower energies.

The total cross section was obtained by integrating the angular distributions. This is presented as a function of energy in Fig. 4. The total cross section is a smoothly varying function increasing quite rapidly, as is characteristic of Coulomb barrier penetrability.

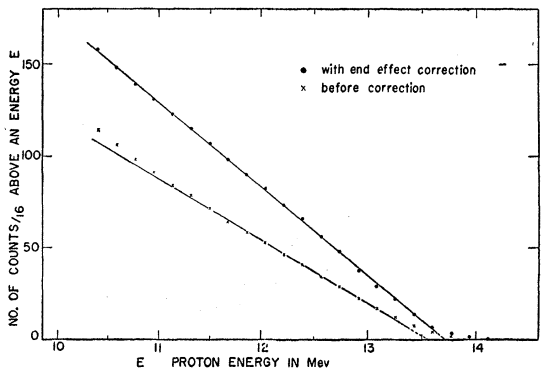


FIG. 2. Integrated recoil proton energy spectrum for the ground-state neutrons. The curves show the result of making the end-effect correction.

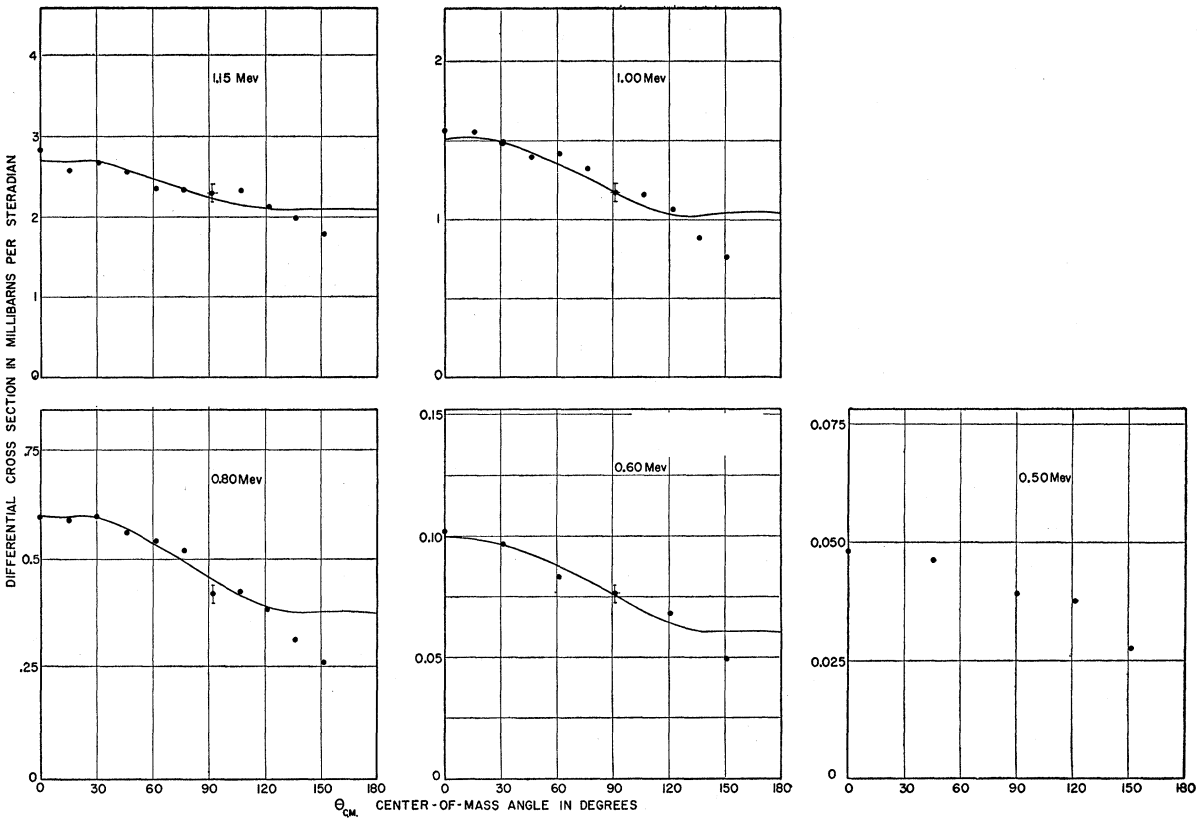


FIG. 3. Angular distributions of ground-state neutrons from $B^{11}(d,n)C^{12}$ reaction for deuteron bombarding energies of 0.5, 0.6, 0.8, 1.00, and 1.15 Mev. Differential cross sections are in millibarns per steradian. Solid curves are fits based on nuclear stripping theory.

## DISCUSSION

The data are consistent with an analysis in terms of compound nucleus formation or in terms of a direct first order interaction similar to the deuteron stripping theory. An analysis[5] of the reaction $B^{11}(d,n)C^{12}$ based on a nuclear stripping theory has been completed for the energy range 0.6 to 4.7 Mev. This particular discussion[5] of the reaction is based upon a Born approximation. The use of a final state wave function for the outgoing neutron which is antisymmetric for the exchange of the neutron from the deuteron and the outer shell neutrons of the $B^{11}$ includes the probability of heavy-particle stripping[3] from the $B^{11}$. The exchange wave function for the final state neutrons also introduces interference between the deuteron stripping and heavy-particle stripping. This interference is large below the Coulomb barrier.

The differential cross section can be written as

$$\frac{d\sigma}{d\Omega}=C(E)\left|G_D(K_1)j_1(k_1R_1)+\frac{\Lambda_2}{\Lambda_1}G_H(K_2)j_0(k_2R_2)\right|^2,$$

where $k_n$= center-of-mass wave number of the outgoing neutron, $k_d$= center-of-mass wave number of the incident deuteron,

$$K_1=[k_n^2+\tfrac{1}{4}k_d^2-k_nk_d\cos\theta]^{\frac{1}{2}},$$

$$k_1=\left[k_d^2+\left(\frac{11}{12}k_n\right)^2-\frac{11}{6}k_nk_d\cos\theta\right]^{\frac{1}{2}},$$

$$K_2=\left[k_n^2+\left(\frac{1}{11}k_d\right)^2+\frac{2}{11}k_nk_d\cos\theta\right]^{\frac{1}{2}},$$

$$k_2=[k_d^2+(\tfrac{1}{6}k_n)^2+\tfrac{1}{3}k_nk_d\cos\theta]^{\frac{1}{2}},$$

$$G_D(K_1)=\frac{2(2\pi\alpha_d)^{\frac{1}{2}}}{\alpha_d^2+K_1^2},$$

$$G_H(K_2)=\left\{\frac{\alpha_B^2}{\alpha_B^2-K_2^2}+\frac{1.9\beta_B^2}{\beta_B^2+K_2^2}\right\}\times\{0.535\sin(K_2r_B)+j_1(K_2r_B)\}.$$

The $j_l(kR)$ terms are the spherical Bessel functions of order $l$.

$\Lambda_2/\Lambda_1$ is proportional to the ratio of the amplitudes of the exchange term and the deuteron stripping term. $\Lambda_2/\Lambda_1$ has been taken as the principal adjustable parameter of this analysis.

[5] G. E. Owen and L. Madansky, Phys. Rev. **105**, 1766 (1957).

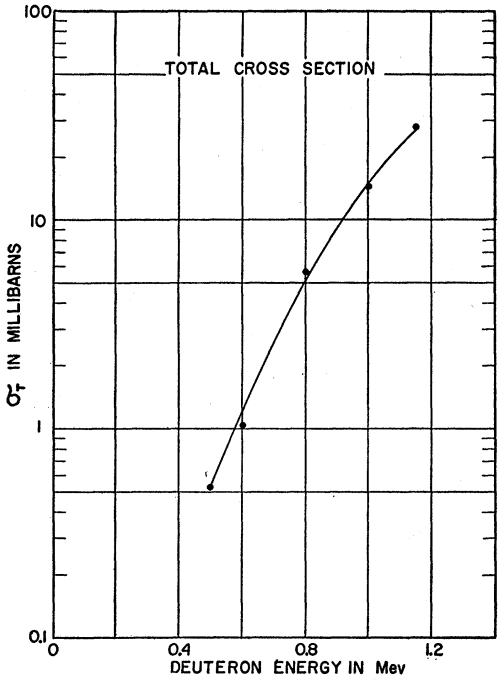


FIG. 4. Total cross sections for the ground-state neutrons from $B^{11}(d,n)C^{12}$. Cross sections are in millibarns. Solid curve is best fit to experimental data.

For simplicity the interaction radii $R_1$ and $R_2$ of the centrifugal barrier terms $j_1(k_1R_1)$ and $j_0(k_2R_2)$ were set equal and held constant for the theoretical curves shown in Fig. 3. The use of the interaction radius is a method of accounting for distortions of the plane waves which are inherent in the Born approximation. Therefore it would not be unreasonable to expect the interaction radii to vary slowly with the energy, particularly below the Coulomb barrier. In fact if the radius $R_1$ is allowed to approach zero for the energies which we are considering, the theoretical curves agree very well with the experiment. This lowering of $R_1$ implies that the Coulomb distortion of the captured wave shifts the first maximum of the probability amplitude away from the origin.

All of the data presented here were fitted with a radius of $3.8\times10^{-13}$ cm, and $A_2/A_1$ was adjusted to give the best fit at 15° and 120° (c.m.). Values of $A_2/A_1$ are to be found in Table I. These values decrease as the energy decreases. The data could also be fitted by an expression of the form $1+a\cos\theta$. Table I shows values of $\sigma_T$, $A_2/A_1$, and the coefficient $a$ at different energies.

Since the center of mass of the deuteron must appear at the surface of the target nucleus for the heavy-particle stripping process (or deuteron capture), one would expect that $A_2/A_1$ would decrease with energy below the Coulomb barrier.

## CONCLUSION

The measured angular distributions show a forward throw at 0.800 Mev, and are more isotropic at 1.15 Mev. This information is particularly interesting in the light of the higher energy experiments performed by Class *et al.*[1]

The calculations based upon an exchange stripping formalism indicate that there is strong positive interference between the forward and backward components just below the Coulomb barrier. This behavior is consistent with the observed experimental isotropy at 1.15 Mev. Further, the amplitude of the backward component might be expected to decrease relative to the amplitude of the forward component in this region. Thus below the region of strong positive interference we could expect to find that the angular distribution is mainly made up of the forward component. This behavior is also consistent with the experimental distributions.

TABLE I. Total cross sections, $A_2/A_1$ and the coefficient $a$ as a function of the incident deuteron energy.

| $E$ (Mev) | $\sigma_T$ (mb) | $A_2/A_1$ | $a$ |
|---|---|---|---|
| 0.5 | 0.53 | ... | 0.25 |
| 0.6 | 1.03 | 0.32 | 0.34 |
| 0.8 | 5.64 | 0.36 | 0.43 |
| 1.0 | 14.4 | 0.43 | 0.33 |
| 1.15 | 28.0 | 0.52 | 0.17 |

The interference term is most important in the behavior of the theoretical curves. The effects must be gross effects, since no attempt has been made to use properly distorted waves.

It must be recognized that theoretical fits have been attempted in regions of high distortion, and that except for the choice of radii, no attempt has been made to use exact wave functions. This approach is reasonable only under the assumption that the variations in the theoretical curves arising from kinematics and interference are larger than the corrections brought about by the distortion of the plane waves.

The authors wish to acknowledge the many helpful discussions and comments of Dr. L. Madansky.